Dalton Transactions

Cite this: *Dalton Trans.*, 2012, **41**, 6189

www.rsc.org/dalton

PAPER

A novel quinoline-based two-photon fluorescent probe for detecting Cd^{2+} *in vitro* and *in vivo*†

Yiming Li,‡[a,b] Hanbao Chong,‡[a] Xiangming Meng,*[a] Shuxin Wang,[a] Manzhou Zhu[a] and Qingxiang Guo[b]

Received 26th January 2012, Accepted 5th April 2012
DOI: 10.1039/c2dt30192j

A new two-photon fluorescent Cd^{2+} probe **APQ** is developed by introducing a N^1,N^1-dimethyl-N^2-(pyridin-2-ylmethyl)ethane-1,2-diamine binding group and a 4-methoxyphenylvinyl conjugation-enhancing group to the 2- and 6-positions of quinoline. This probe shows a large red shift and good emission enhancement under Cd^{2+} binding. It also exhibits a high ion selectivity for Cd^{2+} (especially over Zn^{2+}) and a large two-photon absorption cross section at 710 nm. Two-photon microscopy imaging studies reveal that the new probe is non-toxic and cell-permeable and can be used to detect intracellular Cd^{2+} under two-photon excitation.

Introduction

As one of the most toxic metal pollutants, cadmium has been widely used in industry, agriculture, and many other fields.[1–3] This element is not essential for life and listed by the U.S. Environmental Protection Agency as one of 126 priority pollutants. There have been many reports on the toxicity of Cd^{2+} to bones, kidneys, the nerve system, and tissues, which result in many serious health problems.[4–6] In particular, Cd^{2+} can replace Zn^{2+} in many zinc enzymes, thereby impairing their catalytic activities.[7] Thus, the detection and quantification of Cd^{2+} *in vitro* and *in vivo* is a highly needed technology for a number of research areas. Although several approaches including atomic absorption and inductively coupled plasma have been previously developed for the detection of Cd^{2+},[8–10] these methods are relatively expensive and unsuitable for real-time monitoring. In comparison, fluorescent probes often provide a better choice to detect metal ions in biology and the environment because of their high selectivity and sensitivity.[11–13] Earlier fluorescent Cd^{2+} probes are mostly designed based on single-photon fluorescence technology.[3,6,14–18] Most of these earlier fluorescent Cd^{2+} probes also suffer from relatively low selectivity between Cd^{2+} and Zn^{2+}.[19–22]

Recently, two-photon microscopy (TPM) has evolved into a widely used tool in biomedical research because this technology shows less phototoxity, better spatial localization, increased specimen penetration, and lower cellular autofluorescence.[23–29] Although many two-photon fluorescent probes have been developed for the detection of various analytes, very few studies have been reported about the development of two-photon probes for Cd^{2+}. Herein, we design and synthesize a 6-substituted quinoline-based Cd^{2+} two-photon probe **APQ** (Scheme 1). This design is inspired by our recent success in developing a two-photon Zn^{2+} probe derived from 7-hydroxyquinoline.[30] The reason for using the quinoline skeleton is that quinoline exhibits good two-photon spectrum properties, good water solubility, and low cytotoxicity.[31–33] To enhance the ion selectivity and sensitivity, the *N*,*N*-dimethyl-*N*-(pyridin-2-ylmethyl)methanediamine group is incorporated as a Cd^{2+} receptor. Moreover, we put a 4-methoxyphenylvinyl conjugation-enhancing group at the 6-position to promote intramolecular charge transfer (ICT) to improve the fluorescence properties. This ICT involves a charge transfer process from an electron donor to an electron acceptor within a fluorophore, thereby causing a red-shift emission upon excitation.[34–36]

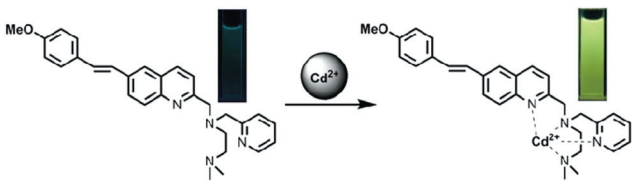

Scheme 1 The design of **APQ** for Cd^{2+} detection.

Experimental section

All reagents and solvents were commercially purchased. ^{1}H NMR spectra were recorded on Bruker-400 MHz spectrometers and ^{13}C NMR spectra were recorded on 100 MHz spectrometers. Fluorescence spectra were obtained using a HITACHI F-2500 spectrometer. The detection of metal ions was operated at pH 7.4, maintained with HEPES buffer (25 mM HEPES/0.1 M

[a]*Department of Chemistry, Anhui University, Hefei 230039, P. R. China. Fax: +86-551-5107342; Tel: +86-551-5108970*
[b]*Department of Chemistry, University of Science and Technology of China, Hefei 230026, P. R. China. E-mail: mengxm@ahu.edu.cn*
†Electronic supplementary information (ESI) available: Details of photophysical measurements and cell imaging; NMR, MALDI-TOF MS spectra data. See DOI: 10.1039/c2dt30192j
‡These authors contributed equally to this work.

$NaNO_3$). UV-vis absorption spectra were recorded on a Techcomp UV 1000 spectrophotometer. Fluorescence responses were recorded on a FL2500. MS spectra were conducted by Bruker MALDI TOF. The two-photon cross section was tested in methanol with 1 mM **APQ**.

6-Bromo-2-methylquinoline (1)

A mixture of 4-bromobenzenamine (14.59 g, 84.8 mmol) and HCl (6 N, 60 mL) was heated to 100 °C. Then, crotonaldehyde (11.9 g, 170 mmol) was added slowly. The resulting mixture was refluxed until TLC showed no raw material. After being cooled to room temperature, 200 mL of H_2O was added. The mixture was extracted with EtOAc (100 mL × 2) to remove unreacted crotonaldehyde. The aqueous phase was neutralized with aqueous ammonia and then extracted with EtOAc (50 mL × 2). The organic phase was dried by Na_2SO_4 and evaporated to give the crude product. The target product was recrystallized in EtOAc–PE to give 13.46 g of **1** (60.64 mmol, yield = 75.6%). ^{1}H NMR (400 MHz, $CDCl_3$, ppm): δ 2.73 (3H, s), 7.29–7.31 (1H, d, J = 8.4 Hz), 7.73–7.75 (1H, d, J = 9.0 Hz), 7.87–7.96 (3H, m). ^{13}C NMR (400 MHz, $CDCl_3$, ppm): δ 25.18, 119.57, 122.91, 127.64, 129.54, 130.12, 133.03, 135.49, 146.05, 159.45.

(E)-6-(4-Methoxystyryl)-2-methylquinoline (2)

A mixture of **1** (6.03 g, 27.15 mmol), 1-methoxy-4-vinylbenzene (4.37 g, 32.58 mmol), $PdCl_2(PPh_3)_2$ (77 mg, 0.97 mmol), K_2CO_3 (11 g, 79.7 mmol) and DMF (25 mL) was heated at 160 °C for 24 h. After being cooled to room temperature, the mixture was filtered to remove salts, and then 100 mL of H_2O was added. The resulting mixture was extracted by dichloromethane (50 mL × 3). The organic phase was combined, dried over Na_2SO_4, and evaporated to give the crude product. The target product was recrystallized in EtOAc–PE to give 6.77 g of **2** (24.63 mmol, yield = 90.7%). ^{1}H-NMR (400 MHz, $CDCl_3$, ppm): δ 2.75 (3H, s), 3.84 (3H, s), 6.91–6.93 (2H, d, J = 8.6 Hz), 7.08–7.21 (2H, q, J = 16.3 Hz), 7.25–7.27 (1H, d, J = 8.3 Hz), 7.48–7.50 (2H, d, J = 8.6 Hz), 7.73 (1H, s), 7.91–7.93 (1H, d, J = 8.9 Hz), 8.01–8.03 (2H, d, J = 8.5 Hz). ^{13}C-NMR (100 MHz, $CDCl_3$, ppm): δ 25.11, 55.35, 114.23, 122.39, 125.19, 125.79, 126.81, 127.39, 127.87, 128.59, 129.36, 129.90, 135.26, 136.35, 147.07, 158.43, 159.54.

(E)-6-(4-Methoxystyryl)quinoline-2-carbaldehyde (3)

A solution of compound **2** (2.00 g, 7.27 mmol) in dioxane (20 mL) was heated at 60 °C. SeO_2 (8.00 mmol, 0.889 g) was added to this solution. Then the reaction temperature was increased to 80 °C. After 2.5 h, the mixture was cooled to room temperature. Precipitates were filtered off and washed with dioxane (5 mL × 2). The organic phase was combined and concentrated to give the crude product. The crude material was purified by column chromatography (dichloromethane as the eluent) to give 1.818 g of **3** (6.61 mmol, yield = 90.9%). ^{1}H NMR (400 MHz, $CDCl_3$, ppm): δ 3.85 (3H, s), 6.92–6.94 (2H, d, J = 8.6 Hz), 7.11–7.30 (2H, dd, J = 16.1 Hz), 7.50–7.52 (2H, d, J = 8.6 Hz), 7.82 (1H, s), 7.99–8.05 (2H, dd, J = 16.4 Hz), 8.18–8.25 (2H, dd, J = 18.1 Hz), 10.21 (1H, s). ^{13}C NMR (100 MHz, $CDCl_3$, ppm): δ 55.37, 114.33, 117.88, 125.11, 125.15, 128.19, 128.30, 129.41, 130.54, 130.64, 131.37, 136.97, 138.71, 147.44, 151.91, 159.97, 193.51.

(E)-N^1-((6-(4-Methoxystyryl)quinolin-2-yl)methyl)-N^2,N^2 dimethyl-N^1-(pyridin-2-ylmethyl)ethane-1,2-diamine (APQ)

1.5 g of compound **3** (5.2 mmol) and 1.0 g of compound **4** (5.2 mmol) were mixed in 50 mL of dichloromethane and stirred for 1 h. Then, 1.33 g of $NaBH(OAc)_3$ (6.24 mmol) was added gradually in 1 h. After 4 h, the solution was washed by 5 mL of water twice. The organic layer was dried by sodium sulfate and evaporated to dryness. The crude product was purified by column chromatography by using a mixed eluent DCM–MeOH (10 : 1). ^{1}H-NMR (400 MHz, DMSO, ppm): δ 8.48–8.47 (1H, d, J = 4.1 Hz), 8.28–8.26(1H, d, J = 8.5 Hz), 8.04–8.02 (1H, dd, J = 1.6, 8.9 Hz), 7.97 (1H, s), 7.93–7.91(1H, d, J = 8.8 Hz), 7.79–7.74 (1H, td, J = 1.7, 7.7, 7.7 Hz), 7.70–7.68 (1H, d, J = 8.49 Hz), 7.60–7.58 (2H, d, J = 8.7 Hz), 7.56–7.54 (1H, d, J = 7.8 Hz), 7.39–7.34 (1H, d, J = 16.4 Hz), 7.28–7.25 (1H, d, J = 12.2 Hz), 7.24–7.22 (1H, d, J = 7.5 Hz), 6.98–6.96 (2H, d, J = 8.7 Hz), 3.93 (2H, s), 3.81 (2H, s), 3.78 (3H, s), 2.63–2.60 (2H, t, J = 6.9 Hz), 2.44–2.40 (2H, t, J = 6.8 Hz), 2.06 (6H, s). ^{13}C NMR (100 MHz, DMSO, ppm) δ 160.04, 159.34, 159.14, 148.65, 146.46, 136.44, 136.05, 135.18, 129.51, 129.27,128.77, 127.93, 127.25, 127.10, 125.42, 125.21, 122.68, 122.05, 121.33, 114.21, 60.73, 60.10, 56.94, 55.12, 51.49, 45.27.

Measurement of two-photon cross section (δ)

Two-photon excitation fluorescence (TPEF) spectra were measured using femtosecond laser pulse and Ti: sapphire system (680–1080 nm, 80 MHz, 140 fs, Chameleon II) as the light source. All measurements were carried out in air at room temperature. Two-photon absorption cross sections were measured using the two-photon-induced fluorescence measurement technique. The two-photon absorption cross sections (δ) were determined by comparing their TPEF to that of fluorescein in different solvents, according to the following equation:

$$\delta = \delta_{\mathrm{ref}} \frac{\Phi_{\mathrm{ref}}}{\Phi} \frac{c_{\mathrm{ref}}}{c} \frac{n_{\mathrm{ref}}}{n} \frac{F}{F_{\mathrm{ref}}}$$

In the equation, the subscript ref stands for the reference molecule. δ is the two-photon adsorption cross-section value, c is the concentration of solution, n is the refractive index of the solution, F is the TPEF integral intensities of the solution emitted at the exciting wavelength, and Φ is the fluorescence quantum yield. The δ_{ref} value of reference was taken from the literature.[37]

Cytotoxicity assays

To test the cytotoxic effect of the probe in cells for over a 24 h period, MTT (5-dimethylthiazol-2-yl-2,5-diphenyltetrazolium bromide) assay was performed as previously reported.[38] HeLa cells were passed and plated to *ca.* 70% confluence in 96-well plates 24 h before treatment. Prior to **APQ** treatment, DMEM

(Dulbecco's Modified Eagle Medium) with 10% FCS (Fetal Calf Serum) was removed and replaced with fresh DMEM, and aliquots of **APQ** stock solutions (5 mM DMSO) were added to obtain final concentrations of 10, 30, and 50 μM, respectively. The treated cells were incubated for 24 h at 37 °C under 5% CO_2. Subsequently, the cells were treated with 5 mg mL^{-1} MTT (40 μL per well) and incubated for an additional 4 h (37 °C, 5% CO_2). Then, the cells were dissolved in DMSO (150 μL per well), and the absorbance at 570 nm was recorded. The cell viability (%) was calculated according to the following equation: Cell viability% = OD_{570}(sample)/OD_{570}(control) × 100, where OD_{570}(sample) represents the optical density of the wells treated with various concentrations of **APQ** and OD_{570}(control) represents that of the wells treated with DMEM plus 10% FCS. The percent of cell survival values is relative to untreated control cells.

Cell culture and two-photon fluorescence microscopy imaging

For two-photon bio-imaging, HeLa cells were cultured in DMEM supplemented with 10% FCS, penicillin (100 μg mL^{-1}), and streptomycin (100 μg mL^{-1}) at 37 °C in a humidified atmosphere with 5% CO_2 and 95% air. Cytotoxicity assays show that **APQ** is safe enough for two-photon bio-imaging at low concentrations, so that the cells were incubated with 15 μM **APQ** at 37 °C under 5% CO_2 for 30 min, washed once and bathed in DMEM containing no FCS prior to imaging and/or Cd^{2+} addition. Then 20 μM Cd^{2+} was added in the growth medium for 0.5 h at 37 °C, washed 3 times with PBS buffer. Then, cells were imaged on a confocal microscope (Zeiss LSM 510 Meta NLO). Two-photon fluorescence microscopy images of labeled cells were obtained by exciting the probe with a mode-locked titanium-sapphire laser source set at wavelength 800 nm.

Results and discussion

As shown in Scheme 2, **APQ** can be easily synthesized in four steps with good yields. With the probe in hand, we then examine its complex with Cd^{2+}. The ^1H NMR spectra of **APQ** (ESI†) show that upon coordination to Cd^{2+} in DMSO-d_6 the proton at the *ortho*-position of pyridine shifts downfield from 3.34 to 3.62 ppm. Job's plot analysis indicates when the Cd^{2+} molar fraction reaches 0.5, the maximum fluorescence intensity is obtained. This indicates a 1 : 1 bonding model between the probe and Cd^{2+}. Furthermore, the MALDI-TOF MS spectrum of the probe increased by 148 Da upon the addition of Cd^{2+}. This observation confirms the formation of the **APQ**–Cd^{2+} complex with a 1 : 1 binding mode (Fig. 1) (ESI†).

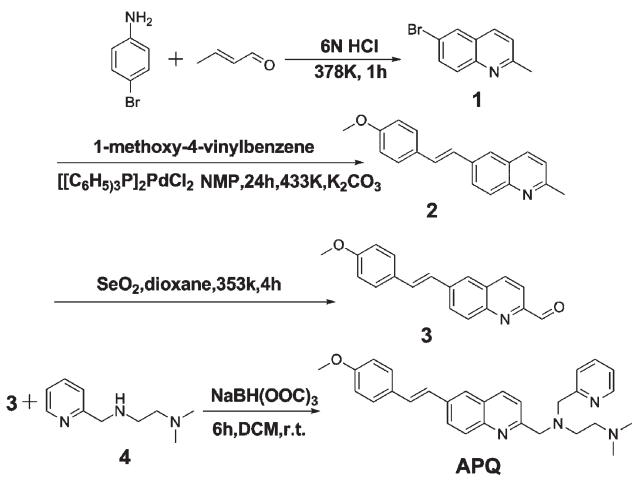

Scheme 2 Synthesis of **APQ**.

Absorption spectra studies

To investigate the binding property of **APQ** toward Cd^{2+}, the UV-vis spectra of **APQ** are measured at room temperature in the Tris-HCl (50 mM, pH = 7.4) ethanol–H_2O (v/v = 1 : 9) buffer in the presence of Cd^{2+}. As shown in Fig. 2, the UV-vis spectrum of **APQ** exhibits two strong absorption peaks at 290 and 340 nm, respectively. Upon addition of Cd^{2+} (0 to 1.5 equiv.), the absorption spectrum of **APQ** exhibits a bathochromic shift with a clear isosbestic point at 310 nm. Besides, **APQ** shows clear absorption shifts in the visible light range 325–375 nm, indicating the electron-donating effect of the 6-methoxylphenyl-vinyl group.

Fluorescence spectra responses

As shown in Fig. 3, **APQ** exhibits a weak fluorescence emission at 475 nm when excited at 360 nm. The addition of Cd^{2+} causes

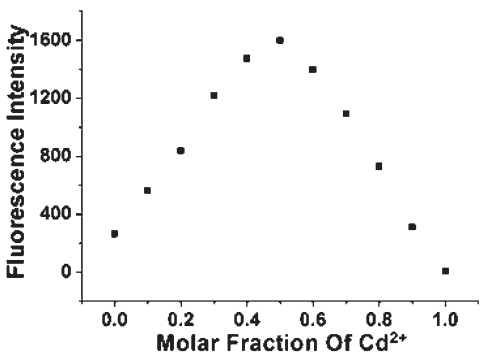

Fig. 1 Job's plot for binding with Cd^{2+} (λ_{ex} = 360 nm, λ_{em} = 520 nm).

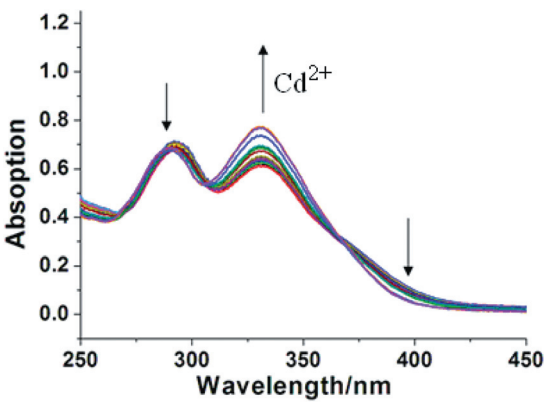

Fig. 2 The UV-vis spectra of **APQ** in the presence of Cd^{2+}.

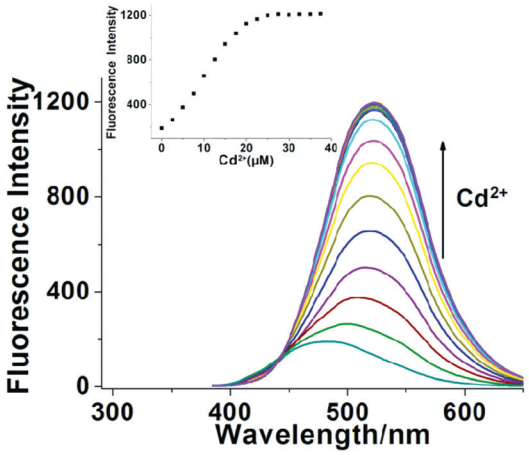

Fig. 3 Fluorescence emission spectra of **APQ** (25 μM), with the excitation at 360 nm, upon the titration of Cd^{2+} (0–1.5 equiv) in methanol–water solution (1 : 9, v/v, 50 mM HEPES buffer, pH = 7.4).

the maximum emission of **APQ** to shift from 475 to 520 nm with a significant red shift of 45 nm. Such a large red shift is rather rare among the fluorescent probes reported for Cd^{2+} detection to date.[18] This red shift also indicates that the nitrogen atom of the quinoline platform is coordinated with Cd^{2+} causing an enhanced ICT effect. Such a large red shift provides a good opportunity for fluorescent Cd^{2+} detection using this new probe. Note that the maximum of fluorescence emission intensity is obtained when the Cd^{2+} concentration equals to that of the probe. This result further verifies that the **APQ**–Cd^{2+} complex is formed by 1 : 1 binding mode.

As to the quantum yield, we find that **APQ** exhibits a quantum yield enhancement of nearly 4-fold (form $\Phi_{free} = 0.057$ to $\Phi_{Cd^{2+}} = 0.2124$) upon binding to Cd^{2+}. The dissociation constant K_d of APQ with Cd^{2+} was tested in PBS (phosphate buffered saline) buffer and calculated to be 2.72×10^{-9} M, suggesting high sensitivity for Cd^{2+}. We conclude that **APQ** can detect free Cd^{2+} in the nanomolar range, and therefore affords sufficient sensitivity for Cd^{2+} detection in living cells.

Ion selectivity and pH stability

Metal ion selectivity is another important character of the fluorescent probe. As shown in Fig. 4, **APQ** can selectively respond between Cd^{2+} and other metal ions in both the fluorescence intensity and emission wavelength shift. Upon addition of 1 equiv. Cd^{2+}, the fluorescence intensity increases by 8.3 fold. Simultaneously, the maximal emission wavelength of **APQ** shifts from 475 nm to 520 nm and this phenomenon is similar as previously reported for quinoline based probes.[39,40] The ion competitive experiments indicate that Ca^{2+}, Cr^{3+}, Cu^{+}, Fe^{2+}, Fe^{3+}, Hg^{2+}, K^{+}, Mg^{2+}, Mn^{2+}, Na^{+}, Pb^{2+}, and more importantly Zn^{2+}, exert little effect on the emission intensity. Moreover, Co^{2+}, Cu^{2+} and Ni^{2+} quench the fluorescence.[28,30] Note that previous Cd^{2+} probes often suffer from low selectivity between Cd^{2+} and Zn^{2+}. By comparison, **APQ** can be considered as a good candidate for monitoring Cd^{2+} flux in biological systems.

Furthermore, we examined the pH-dependence of **APQ** and its Cd^{2+} complex (Fig. 5). In the biologically relevant pH range

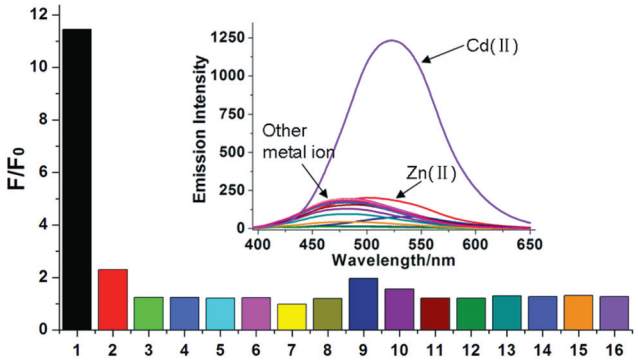

Fig. 4 Fluorescence response of **APQ** to different metal ions (1–16: Cd^{2+}, Zn^{2+}, Ca^{2+}, Co^{2+}, Cr^{3+}, Cu^{+}, Cu^{2+}, Fe^{2+}, Fe^{3+}, Hg^{2+}, K^{+}, Mg^{2+}, Mn^{2+}, Na^{+} Ni^{2+}, Pb^{2+}) in Tris buffer (pH = 7.4, λ_{ex} = 360 nm). Insert: emission spectra of **APQ** upon addition of Cd^{2+} and other metal ions (λ_{ex} = 360 nm).

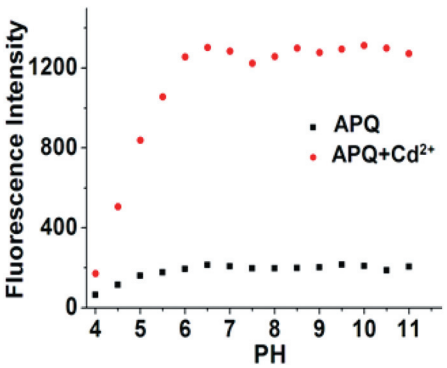

Fig. 5 pH sensitivity of **APQ** and its Cd^{2+} complex.

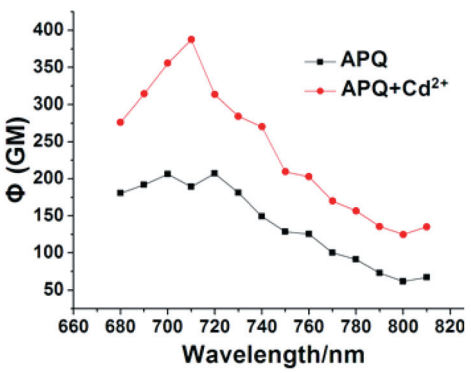

Fig. 6 Two-photon excitation spectra of **APQ** with and without Cd^{2+}.

(*e.g.* 5–9), the fluorescence intensity of **APQ** and the **APQ**–Cd^{2+} complex are found to be almost pH insensitive. This phenomenon indicates that pH changes do not affect the fluorescence signal output of **APQ**-Cd^{2+} under physiological conditions and, therefore, expands its application to physiological studies.

Two-photon cross sections

We further determine the two-photon cross sections of **APQ** and its Cd^{2+} complexes using the two-photon induced fluorescence measurement technique. As shown in Fig. 6, **APQ** shows the δ_{max} value of 206 GM at 720 nm. Upon addition of 1.2 equiv. of

Cd^{2+}, the δ_{max} value increases by about 200 GM. It is critical to point out that the above two-photon cross section values are significantly larger than the previously reported ones for other Cd^{2+} probes. Therefore, **APQ** with an enlarged two-photon cross section should act as a valuable tool to image Cd^{2+} flux in living systems under two-photon excitation.

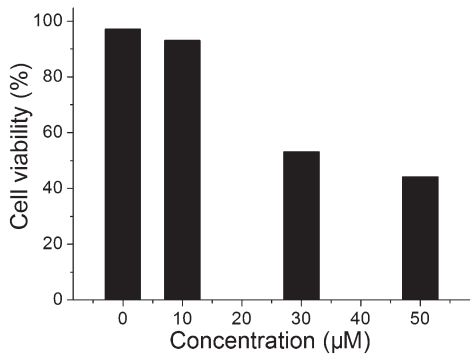

Fig. 7 Cytotoxicity data of **APQ** (HeLa cells incubated for 24 h).

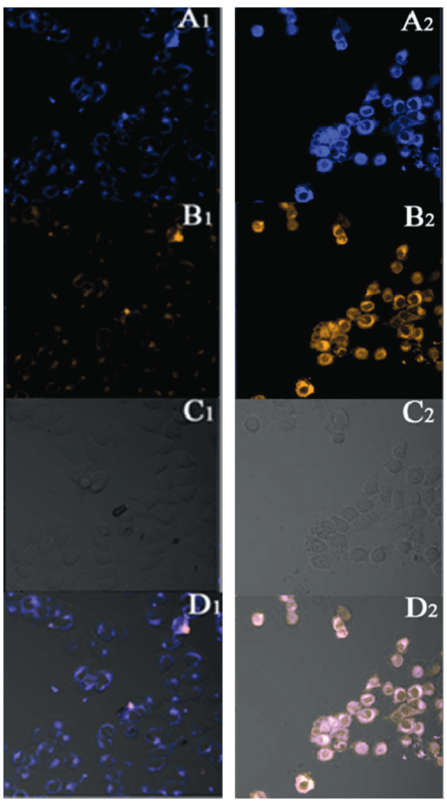

Fig. 8 Two-photon image of Hela cells labeled with 20 μM **APQ** after 30 min of incubation, washed with PBS buffer. λ_{ex} = 800 nm. (A_1) Emission wavelength from 450 to 480 nm; (B_1) Emission wavelength from 510 to 540 nm; (C_1) Bright-field of HeLa cells; (D_1) The overlay of A_1 and B_1. TPF image of **APQ** labeled HeLa after 0.5 h treated with 20 μM $CdCl_2$ water solution, λ_{ex} = 800 nm. (A_2) Emission wavelength from 450 to 480 nm; (B_2) Emission wavelength from 510 to 540 nm; (C_2) Bright-field of HeLa cells; (D_2) The overlay of A_2 and B_2.

Cell cytotoxicity and two-photon bio-imaging

Cytotoxicity is a potential side effect of many organic probes when used in living cells or tissues. The use of a fluorescent probe in biological systems must meet the criterion that the probe should not interact or interfere with the biological system. To this end, we conduct cytotoxic assays in HeLa cells for **APQ**. As shown in Fig. 7, MTT assay demonstrates that the cell viability remains more than 90% after being treated with 10 μM **APQ**. As a result, **APQ** show little cytotoxicity for long period incubation and should be safe when used for two-photon bio-imaging.

Finally, we investigate the utility of **APQ** for monitoring the intracellular Cd^{2+} flux under two-photon excitation. HeLa cells are cultured and stained with **APQ** within 30 min and washed once in DMEM containing no FCS prior to imaging or Cd^{2+} addition. TPM images are obtained by exciting the probe at wavelength 800 nm. As shown in Fig. 8, because **APQ** can penetrate the cell membrane, before the addition of Cd^{2+} **APQ**-labeled HeLa cells display very weak intracellular fluorescence. The system then exhibits a greatly increased fluorescence both from optical windows at 450–480 nm and 510–540 nm upon the addition of Cd^{2+} (20 μM) within 0.5 h. These findings clearly demonstrate that our new probe can readily reveal the variation of intracellular Cd^{2+} flux under two-photon excitation.

Note that we recently also developed two highly selective two-photon zinc probes **6-MPVQ** and **6-MPQ** (Fig. 9a). They were designed and synthesized based on an identical lumophore coupled to a different ligand.[41] To explain the selectivity observed for the different probes, we have tested the selectivity of **APQ** between Cd^{2+} and Zn^{2+} by MALDI-TOF mass. The

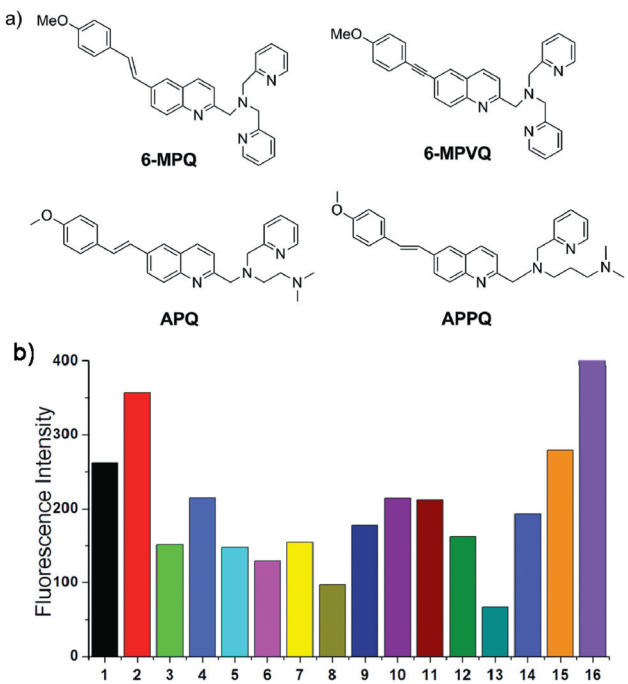

Fig. 9 (a) Structure of **6-MPQ**, **6-MPVQ**, **APQ** and **APPQ**; (b) fluorescence response of **APPQ** to different metal ions (1–16: Ca^{2+}, Cd^{2+}, Co^{2+}, Cr^{3+}, Cu^{+}, Fe^{2+}, Fe^{3+}, Hg^{2+}, K^{+}, Mg^{2+}, Mn^{2+}, Na^{+} Ni^{2+}, Pb^{2+}, Zn^{2+}, Ag^{+}) in Tris buffer (pH = 7.4, λ_{ex} = 360 nm).

results verified that **APQ** favors Cd^{2+} over Zn^{2+}, consistent with the binding experiments. Specifically, as shown in Fig. S3 in the ESI,† **APQ** is fully converted to the **APQ**–Cd^{2+} complex in the presence of Cd^{2+} and Zn^{2+}. On the other hand, the binding between **APQ** and Zn^{2+} is relatively weak when only Zn^{2+} is added (Fig. S4†).

To further understand the ion selectivity, we have synthesized another compound **APPQ** with an identical lumophore coupled to a more flexible binding group. As shown in Fig. 9b, **APPQ** can bind to Ag^{2+} the most strongly. Cd^{2+} and Zn^{2+} can also bind to **APPQ**, but both with lower strengths. Therefore, the structure of the binding group indeed exerts a strong influence on ion selectivity.

In theory, the atomic radius of Zn^{2+} is smaller than that of Cd^{2+} and therefore, Cd^{2+} is more sensitive to the steric effect than Zn^{2+}. On the other hand, the d orbitals of Cd^{2+} are more diffused than those of Zn^{2+}, making Cd^{2+} more electron-deficient and more sensitive to the electronic effects than Zn^{2+}. Thus, Zn^{2+} tends to coordinate with a rigid ligand like **6-MPQ**, whereas Cd^{2+} favors the coordination with the more electron-donating and more flexible **APQ** ligand.

Conclusion

In conclusion, we have designed and developed a 6-substituted quinoline-based two-photon Cd^{2+} probe (**APQ**) and investigated its two-photon activities *in vitro* and *in vivo*. The new probe shows a large red shift upon Cd^{2+} binding with 8-fold emission enhancement. Importantly, **APQ** exhibits high ion selectivity and sensitivity for Cd^{2+}, especially to discriminate Cd^{2+} from Zn^{2+}. Compared with previous reported Cd^{2+} probes, **APQ** exhibits a large two-photon cross section of *ca.* 400 GM. Finally, *in vivo* two-photon microscopy imaging demonstrates that the new probe is cell permeable and can act as a good tool to monitor the Cd^{2+} flux in living cells.

Acknowledgements

This study was supported by NSFC (21102002, 20932006 and 21102083), Natural Science Foundation of Education Department of Anhui Province (KJ2010A028, KJ2011A018), and 211 Project of Anhui University.

Notes and references

1 N. D. Lyn Patrick, *Altern. Med. Rev.*, 2003, **8**, 106.
2 L. Pari, P. Murugavel, S. L. Sitasawad and K. S. Kumar, *Life Sci.*, 2007, **80**, 650.
3 Q. Zhao, R. F. Li, S. K. Xing, X. M. Liu, T. L. Hu and X. H. Bu, *Inorg. Chem.*, 2011, **50**, 10041.
4 S. Satarug and M. R. Moore, *Environ. Health Perspect.*, 2004, **112**, 1099.
5 M. Waisberg, P. Joseph and B. Hale, *Toxicology*, 2003, **192**, 95.
6 M. Mameli, M. C. Aragoni, M. Arca, C. Caltagirone, F. Demartin, G. Farruggia, G. De Filippo, F. A. Devillanova, A. Garau, F. Isaia, V. Lippolis, S. Murgia, L. Prodi, A. Pintus and N. Zaccheroni, *Chem.–Eur. J.*, 2010, **16**, 919.
7 N. Saleh, A. M. Rawashdeh, Y. A. Yousef and Y. A. Al-Soud, *Spectrochim. Acta, Part A*, 2007, **68**, 728.
8 A. N. Anthemidis and C. P. Karapatouchas, *Microchim. Acta*, 2008, **160**, 455.
9 G. Kaya and M. Yaman, *Talanta*, 2008, **75**, 1127.
10 A. C. Davis, C. P. Calloway Jr. and B. T. Jones, *Talanta*, 2007, **71**, 1144.
11 E. Tomat and S. J. Lippard, *Curr. Opin. Chem. Biol.*, 2010, **14**, 225.
12 J. W. Lichtman and J. A. Conchello, *Nat. Methods*, 2005, **2**, 910.
13 R. McRae, P. Bagchi, S. Sumalekshmy and C. J. Fahrni, *Chem. Rev.*, 2009, **109**, 4780.
14 G. M. Cockrell, G. Zhang, D. G. VanDerveer, R. P. Thummel and R. D. Hancock, *J. Am. Chem. Soc.*, 2008, **130**, 1420.
15 H. Tian, B. Li, J. Zhu, H. Wang, Y. Li, J. Xu, J. Wang, W. Wang, Z. Sun, W. Liu, X. Huang, X. Yan, Q. Wang, X. Yao and Y. Tang, *Dalton Trans.*, 2012, **41**, 2060.
16 J. X. Peng, J. Du, J. Wang, Y. Wu, J. Zhao, S. Sun and T. Xu, *J. Am. Chem. Soc.*, 2007, **129**, 1500.
17 T. Cheng, Y. Xu, S. Zhang, W. Zhu, X. Qian and L. Duan, *J. Am. Chem. Soc.*, 2008, **130**, 16160.
18 M. Taki, M. Desaki, A. Ojida, S. Iyoshi, T. Hirayama, I. Hamachi and Y. Yamamoto, *J. Am. Chem. Soc.*, 2008, **130**, 12564.
19 E. M. Nolan, J. W. Ryu, J. Jaworski, R. P. Feazell, M. Sheng and S. J. Lippard, *J. Am. Chem. Soc.*, 2006, **128**, 15517.
20 K. Komatsu, K. Kikuchi, H. Kojima, Y. Urano and T. Nagano, *J. Am. Chem. Soc.*, 2005, **127**, 10197.
21 S. Aoki, D. Kagata, M. Shiro, K. Takeda and E. Kimura, *J. Am. Chem. Soc.*, 2004, **126**, 13377.
22 N. J. Williams, W. Gan, J. H. Reibenspies and R. D. Hancock, *Inorg. Chem.*, 2009, **48**, 1407.
23 W. Denk, J. H. Strickler and W. W. Webb, *Science*, 1990, **248**, 73.
24 W. R. Zipfel, R. M. Williams and W. W. Webb, *Nat. Biotechnol.*, 2003, **21**, 1369.
25 F. Helmchen and W. Denk, *Nat. Methods*, 2005, **2**, 932.
26 H. M. Kim and B. R. Cho, *Acc. Chem. Res.*, 2009, **42**, 863.
27 M. Taki, J. L. Wolford and T. V. O'Halloran, *J. Am. Chem. Soc.*, 2004, **126**, 712.
28 Y. Zhang, X. Guo, W. Si, L. Jia and X. H. Qian, *Org. Lett.*, 2008, **10**, 473.
29 L. Xue, Z. J. Fang, G. P. Li, H. H. Wang and H. Jiang, *Sens. Actuators, B*, 2011, **156**, 410.
30 X. Y. Chen, J. Shi, Y. M. Li, F. L. Wang, X. Wu, Q. X. Guo and L. Liu, *Org. Lett.*, 2009, **11**, 4426.
31 L. Xue, H. H. Wang and H. Jiang, *Inorg. Chem.*, 2008, **47**, 43108.
32 L. Xue, C. Liu and H. Jiang, *Org. Lett.*, 2009, **11**, 1655.
33 H. Y. Zhao, Y. M. Li, T. J. Gong and Q. X. Guo, *Chin. Chem. Lett.*, 2011, **22**, 1013.
34 L. Xue, C. Liu and H. Jiang, *Chem. Commun.*, 2009, 1061.
35 A. P. de Silva, H. Q. Nimal Gunaratne, T. Gunnlaugsson, A. J. M. Huxley, C. P. McCoy, J. T. Rademacher and T. E. Rice, *Chem. Rev.*, 1997, **97**, 1515.
36 Z. R. Grabowski and K. Rotkiewicz, *Chem. Rev.*, 2003, **103**, 3899.
37 O. Varnavski, T. Goodson, L. Sukhomlinova and R. Twieg, *J. Phys. Chem. B*, 2004, **108**, 10484.
38 W. Lin, B. Mohandas, C. P. Fontaine and R. A. Colvin, *BioMetals*, 2006, **20**, 891.
39 X. J. Peng, Y. Q. Yu, S. G. Sun, Y. K. Wu and J. L. Fan, *Org. Biomol. Chem.*, 2007, **5**, 226.
40 F. Qian, C. L. Zhang, Y. M. Zhang, W. J. He, X. Gao, P. Hu and Z. J. Guo, *J. Am. Chem. Soc.*, 2009, **131**, 1460.
41 X. M. Meng, S. X. Wang, Y. M. Li, M. Z. Zhu and Q. X. Guo, *Chem. Commun.*, 2012, **48**, 4196.